Cancer Chemother Pharmacol (2005) 55: 101–109
DOI 10.1007/s00280-004-0866-2

ORIGINAL ARTICLE

T. S. Garimella · D. D. Ross · J. L. Eiseman
J. T. Mondick · E. Joseph · T. Nakanishi · S. E. Bates
K. S. Bauer

Plasma pharmacokinetics and tissue distribution of the breast cancer resistance protein (BCRP/ABCG2) inhibitor fumitremorgin C in SCID mice bearing T8 tumors

Received: 25 February 2004 / Accepted: 25 May 2004 / Published online: 1 October 2004

Abstract Multidrug resistance (MDR) remains a major obstacle in the treatment of human cancers. The recently discovered breast cancer resistance protein (BCRP/ABCG2) has been found to be an important mediator of chemotherapeutic MDR. Fumitremorgin C (FTC) is a selective and potent inhibitor of BCRP that completely inhibits and reverses BCRP-mediated resistance at micromolar concentrations. We report a study of the pharmacokinetics and tissue distribution of FTC when administered intravenously (IV) at a dose of 25 mg/kg to female SCID mice bearing the BCRP-overexpressing human ovarian xenograft Igrov1/T8 tumors. Plasma pharmacokinetics and tissue distribution of FTC in various organs and tissues were studied. In addition, the effect of FTC administration on the expression of BCRP in T8 tumors was also assessed by RT-PCR. Administration of a single FTC IV dose did not appear to cause any major toxicities. The resulting pharmacokinetic data were fit to a two-compartment model using NONMEM and the FTC clearance was determined to be 0.55 ml/min (25.0 ml/min/kg) with a 56% inter-animal variability. Area under the plasma concentration time curve was determined by Bailer's method and was calculated to be 1128 ± 111 μg min/ml. FTC was widely distributed in all tissues assayed with highest concentrations found in lungs, liver and kidney in decreasing order, respectively. FTC did not appear to have any effect on the expression of BCRP in T8 tumors. Less than 2% of the administered dose was recovered in the urine and feces after 24 h, suggesting hepatic metabolism as a primary mechanism of elimination. The current study can be used as a basis for future animal or in vivo studies with FTC designed to further understand the impact of BCRP on drug resistance.

Keywords Fumitremorgin C · Breast cancer resistance protein · Multidrug resistance

T. S. Garimella · J. T. Mondick
Department of Pharmaceutical Sciences,
University of Maryland at Baltimore, Baltimore, MD, USA

D. D. Ross · T. Nakanishi · K. S. Bauer
Greenebaum Cancer Center,
University of Maryland School of Medicine,
University of Maryland at Baltimore, Baltimore, MD, USA

D. D. Ross
Baltimore Veterans Affairs Medical Center,
Baltimore, MD, USA

J. L. Eiseman · E. Joseph
University of Pittsburgh Cancer Institute and
Department of Pharmacology, School of Medicine,
University of Pittsburgh, Pittsburgh, USA

S. E. Bates
Cancer Therapeutics Branch, Center for Cancer Research,
National Cancer Institute, Bethesda, MD, USA

K. S. Bauer (✉)
Department of Pharmacy Practice and Science, School of Pharmacy, University of Maryland at Baltimore, Baltimore, MD, USA
E-mail: kbauer@rx-umaryland.edu
Tel.: +1-410-7063274
Fax: +1-410-7066580

Introduction

Multidrug resistance (MDR) remains a major obstacle in the treatment of human cancers. The ATP-binding cassette (ABC) family of transport proteins such as P-glycoprotein (Pgp), the MDR-associated protein subfamily (MRPs) and the breast cancer resistance protein (BCRP/ABCG2/MXR) have the potential to play an important role in MDR. Resistance of cancer cells to multiple drugs is associated with overexpression of these ABC proteins leading to reduced intracellular drug accumulation and clinical treatment failure [21].

The recently discovered ABC half-transporter, BCRP [5], is an important mediator of MDR and can confer resistance to a mixed group of drugs including mitoxantrone [5], camptothecins, doxorubicin, daunorubicin [1], and flavopiridol [20], although significant resistance to anthracyclines is only found following a point mutation in the third transmembrane segment [8]. BCRP

along with conferring resistance to a variety of anticancer agents is also present in a large number of normal human tissues [13], and also in the human brain microvessel endothelium at levels lower than those of Pgp [4]. Human BCRP has recently been implicated in resistance to sterol, steroid and estrogen receptor antagonists that are used in breast cancer treatment [9]. Also there are reports that BCRP is involved physiologically in transport or cellular efflux of photosensitizing porphyrins [10]. BCRP has also been implicated in reducing the oral bioavailability of topotecan [12].

Fumitremorgin C (FTC) has been recently discovered to be a specific and selective inhibitor of BCRP [7, 18, 19]. FTC was identified as a BCRP inhibitor when Rabindran et al. tested a library of extracts from a variety of microorganisms in a cell-based transport screen. One of the extracts from the medium of *Aspergillus* was found to be active and increased the cytotoxicity of mitoxantrone when used in combination. When studied further the pharmacologically active ingredient in the extract was found to be a diketopiperazine, FTC (Fig. 1) [18]. FTC is relatively non-toxic and is able to completely inhibit resistance in cell lines with the highest levels of BCRP-mediated resistance at micromolar concentrations (1–5 μM; 0.38–1.9 μg/ml). The fact that FTC does not reverse resistance to Pgp or MRP1, unlike other inhibitors, makes FTC a potent and selective pharmacologic tool to evaluate the role of BCRP in MDR and to study the impact of BCRP as a drug transporter in drug disposition. To date there have been no studies performed to evaluate the pharmacokinetics and biodistribution of FTC. We therefore undertook studies to determine the pharmacokinetics and tissue distribution of FTC in SCID mice bearing BCRP-expressing human ovarian carcinoma Igrov1/T8 tumor and also to study the effect of FTC on the levels of BCRP expressed in the tumor.

Materials and methods

Drugs and additives

FTC (Fig. 1) was isolated by the Natural Products Support Group, National Cancer Institute (NCI).

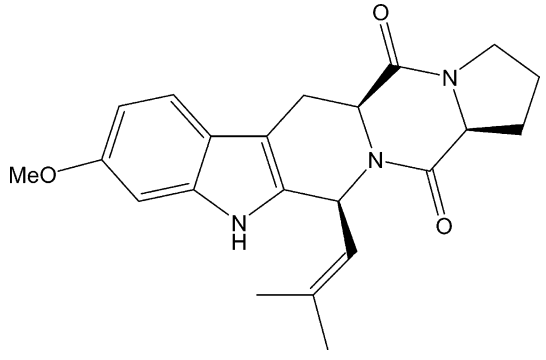

Fig. 1 Structure of FTC

Roquefortine (the internal standard for the FTC assay) was obtained from Sigma Chemical Company (St Louis, Mo.). Cremophor EL, USP ethyl alcohol, and USP 0.9% sodium chloride for injection were obtained, respectively, from Sigma Chemical Company, Pharmaco Products (Brookfield, Ct.) and Baxter (Deerfield, Ill.). HPLC grade methanol and acetonitrile were obtained from B&J (Muskegon, Mich.).

Mice and tumor growth

Mice

Specific-pathogen-free adult CB-17 female SCID mice (5–6 weeks of age) were obtained from the animal program administered by the Biological Testing Branch of the National Cancer Institute. Mice were handled in accordance with the Guide for the Care and Use of Laboratory Animals (National Research Council, 1996) and a protocol approved by the Institutional Animal Care and Use Committee of the University of Pittsburgh. Mice were given at least 1 week to acclimate to the animal facility before they were studied. To minimize exogenous infection, mice were maintained in sterile microisolator cages. Ventilation and airflow in the animal facility were set to 12 changes per hour. Room temperatures were regulated at 72 ± 2°F, and the rooms were kept on automatic 12-h light/dark cycles. Mice received Prolab ISOPRO RMH 3000, Irradiated Lab Diet (PMI Nutrition International, Brentwood, Mo.) and sterile water ad libitum. However, on the evening prior to study, food was removed at approximately 6 p.m. and withheld until 4 h after dosing on the next day. Sentinel mice, housed in 20% dirty bedding from study mice, remained murine antibody profile-negative using Assessment + (Charles River Laboratories, Wilmington, Mass.), indicating that the study mice were specific-pathogen-free.

Tumor cell line

The Igrov1/T8 human ovarian cancer cells were obtained from Maliepaard and colleagues [14]. These cells, overexpressing BCRP, were created by selection of Igrov1 cells with topotecan and maintained as described. The cells were expanded in culture in RPMI 1640 medium (Gibco, InVitrogen Corporation, Carlsbad, Calif.) supplemented with 10% fetal bovine serum (Biofluids, Rockville, Md.) and 10 μg/ml gentamicin (Gibco, InVitrogen) and were maintained at 37°C in an incubator under an atmosphere of 95% air and 5% CO_2 at 95% humidity. Before implantation into study animals, cells (5×10^6 cells/mouse) were injected subcutaneously into the right flanks of "passage" SCID mice. Tumor volumes, in cubic millimeters, were calculated twice weekly using the formula $\mathrm{Vol} = L(W^2/2)$ and measurements of length (L) and width (W) obtained by digital caliper. When the tumors in the

passage mice reached approximately 500–1000 mm^3, the mice were killed, and the tumors were removed using sterile technique. Tumors were cut into fragments of approximately 25 mg, and the fragments were placed in sterile medium until implantation in study mice. Tumor fragments were implanted subcutaneously into the right flank of the study mice and allowed to grow until the tumor volumes were greater than 100 mm^3, at which time the mice were stratified into groups (each group having three animals) by body weight and tumor volume.

Toxicity

As no prior information regarding the acute toxicity of FTC after intravenous (IV) administration to mice was available for initial experiments, FTC was dissolved at its maximal solubility of 2.5 mg/ml in the dosing solution ethanol/Cremophor EL/saline (1:1:6) and animals were dosed with 25 mg/kg. FTC (25 mg/kg) was administered to non-tumor-bearing CB-17 female SCID mice as a single IV dose and the mice were followed for 15 days after dosing to determine any delayed toxicity. Body weights and clinical observations were recorded twice weekly.

Pharmacokinetic sampling

Three mice per time point were killed by CO_2 inhalation, and blood was collected by cardiac puncture using heparinized syringes at the following times after dosing: 5, 10, 15, 30, 45, 60, 120, 180, 240, 360, 420, 960, and 1440 min or 5 min after the administration of vehicle. Blood was transferred to microcentrifuge tubes and stored on ice until centrifuged at 13,000 *g* for 4 min to obtain plasma and red blood cells. Livers, kidneys, hearts, lungs, spleens, brains, fat, skeletal muscles, and tumors were rapidly dissected, placed on ice, weighed, transferred to cryovials, and snap-frozen in liquid nitrogen. Tumors were cut into two pieces, and each piece was weighed prior to placing in the cryovials. Plasma and tissues were stored at −70°C until analysis by HPLC as described below. Urine and feces were collected from animals housed in metabolic cages from the time of dosing until the time they were killed at 24 h (1440 min) after dosing.

Analysis of FTC

FTC plasma concentrations were measured using a newly developed and validated HPLC assay method. Briefly, 100 µl plasma was precipitated with 500 µl acetonitrile containing 300 ng/ml of roquefortine as the internal standard. The mixture was vortexed and centrifuged at 19,000 *g* at 4°C for 10 min. After centrifugation, samples were dried under a stream of nitrogen gas and reconstituted with 100 µl of starting mobile phase, and 80 µl of this mixture was injected into a Hewlett Packard 1100 series HPLC with a DAD detector employing a Waters 4 µm Nova-Pak C18 3.9×150 mm column. The mobile phase of 10 m*M* acetate buffer (pH 4) and acetonitrile (70:30, v/v) was pumped isocratically at a rate of 1 ml/min. FTC was detected by UV absorption at 225 nm and the internal standard roquefortine was detected at 312 nm.

An assay based on the plasma assay was developed for the Igrov1/T8 human tumor xenograft and for the following mouse tissues: brain, liver, kidney, spleen, lung, heart, skeletal muscle, and fat. Tissue samples were similarly analyzed except for the following differences. Tissues were homogenized in a Polytron homogenizer (Brinkman Instruments, Westbury, N.Y.) using phosphate-buffered saline (PBS) (pH 7.4) in a ratio of 1:1 w/v for brain, tumor, lung, fat and kidney, 1:2 w/v for spleen, and 1:3 w/v for heart and skeletal muscle. The homogenization ratios with PBS were different for some of the tissues to allow optimal extraction of the drug. For tumor, liver, kidney, heart, and fat a 100-mg sample was weighed and processed, for brain and skeletal muscle a 200-mg sample was weighed and processed, for spleen a 75-mg sample was weighed and processed and for lung, a 25-mg sample was processed.

The limit of quantitation of FTC was 0.03 µg/ml in plasma and 0.0075 µg/g in tissues. The assay was linear over the range 0.03–30 µg/ml in plasma and 0.0075–120 µg/g in tissues. The range for brain and skeletal muscle was 0.0075–5 µg/g; for fat, heart, tumor, kidney and liver 0.03–10 µg/g; for lung 0.06–120 µg/g; and for spleen 0.02–13.3 µg/g. The newly developed HPLC method yielded retention times of 9.5 min and 13 min for FTC and the internal standard, respectively, for plasma analysis. Drug recovery from spiked samples of plasma was approximately 90%. The intraassay and interassay error of accuracy was less than 14% and 7%, respectively, for the plasma standard curve.

Pharmacokinetic analysis

Pharmacokinetic models were fit to FTC plasma concentration data using the Nonlinear Mixed Effects Modeling Program (NONMEM) version V (Globomax Service Group, Hanover, Md.). Two-compartment and three-compartment pharmacokinetic models with first-order elimination were specified using the NONMEM PREDP subroutines ADVAN3/TRANS4 and ADVAN11/TRANS4, respectively. The FTC pharmacokinetic parameters estimated were the volume of distribution of the central compartment (V_1), clearance from the central compartment (CL), volume of distribution of the peripheral compartment (V_2), and the

intercompartmental clearance (Q). Interanimal variability in pharmacokinetic parameters was estimated by the exponential error model:

$$P_i = \theta \exp(\eta_i) \quad (1)$$

where θ is the population mean value for parameter P, P_i, is the individual parameter estimate, and η_i is a random variable with a mean of zero and a variance of Ω^2 which describes the deviation of P_i from P. Residual variability for FTC pharmacokinetics was modeled by a proportional error model:

$$C_{obs} = C_{pred}(1 + \varepsilon_1) \quad (2)$$

where C_{obs} is the observed concentration, C_{pred} is the model-predicted concentration, and ϵ_1 is the proportional error component. The proportional error component was fixed to the highest variability in the FTC assay so that parameter identifiability was possible a posteriori using a nested error model given the single sample from each animal (destructive sampling). The Akaike information criteria (AIC) was used for compartmental model selection.

Area under the concentration curves

Tissue and plasma area under the curve from 0 min to 1440 min (AUC_{0-1440}) was determined using Bailer's method [2]. This method permits calculation of the variance associated with the AUC, thus yielding a 95% confidence interval (95% CI). Equation 3 was used to calculate the AUC:

$$(AUC_j) = \sum_{q=1}^{m} c_q \bar{y}_{j,q} \quad (3)$$

where $c_q = (1/2)D_2$ for $q = 1$, $(1/2)(D_q + D_{q+1})$ for $q = 2$ to $q = m-1$, $c_q = (1/2)D_m$ for $q = m$; j is the number of groups, D is the time interval, m is the number of time points, and q is any given time point from 1 to m, and $\bar{y}_{j,q}$ is the sample mean of the response at time q in group j. In our case the number of groups $j = 1$. The variance associated with the AUC was calculated using Eq. 4:

$$s^2(AUC_j) = \sum_{q=1}^{m} c_q^2 \left[\frac{s_{jq}^2}{n_{jq}}\right] \quad (4)$$

where s_{jq}^2 is the variance associated with the response for each group at time point q, and n_{jq} is the number of animals per group at time point q. Clearance was estimated for the Bailer-calculated AUC by using Eq. 5:

$$CL = \frac{Dose}{AUC} \quad (5)$$

The maximum concentration (C_{max}) and time of maximum concentration were the observed values.

RT-PCR for BCRP levels in tumor

Isolation of total RNA from T8 tumor xenograft tissue; RT-PCR

Total cellular RNA was isolated from approximately 10 mg of T8 tumor tissue excised from tumor xenografts in the mice, frozen in liquid nitrogen using RNeasy (Qiagen, Valencia, Calif.), according to the manufacturer's protocol. Briefly, solid tumor tissue was homogenized with lysis buffer and total RNA was immediately stabilized. Then, RNA was separated on a silica-gel column and, additionally, treated with DNase I (Qiagen) on the same column. Finally, the RNA was dissolved in water. As a control, total RNA was also isolated from the human ovarian carcinoma lines Igrov1 (parental) and BCRP-overexpressing Igrov1/T8, grown in tissue culture, in vitro. BCRP and β-actin mRNA expression in the tumor samples and cell lines was determined from total cellular RNA, using quantitative, real-time RT-PCR methodology, as described previously [16].

Results

Toxicity

Both groups of animals (FTC-treated and vehicle-treated) exhibited symptoms of ethanol intoxication at about 5 min after administration. The animals did not move and when forced to move, had difficulty controlling their movement and swayed back and forth. Mice receiving FTC at 25 mg/kg IV had rasping and slow respiration for the first 15 min after dosing. By 15 min after dosing all animals had returned to normal activity. FTC-dosed animals were similar to the vehicle control animals in terms of clinical observations and body weights during the 15 days following dosing. Further, when the animals were killed 15 days after administration of FTC, no gross pathology was noted and all tissues appeared normal.

Plasma pharmacokinetics

After IV administration of FTC to female SCID mice bearing Igrov1/T8 tumors, plasma FTC concentrations declined rapidly but were still detectable at the last time point (24 h). A two-compartment open model best described the time-course of FTC in plasma (Fig. 2). Table 1 summarizes the pharmacokinetic parameters obtained from fitting the two-compartment model to the data using NONMEM. There was no significant drop in the value of the minimum objective function and the AIC by fitting a three-compartment model to the data. Thus, parameters for the two-compartment model are presented and 95% CI were calculated for each parameter based on the asymptotic standard errors reported by

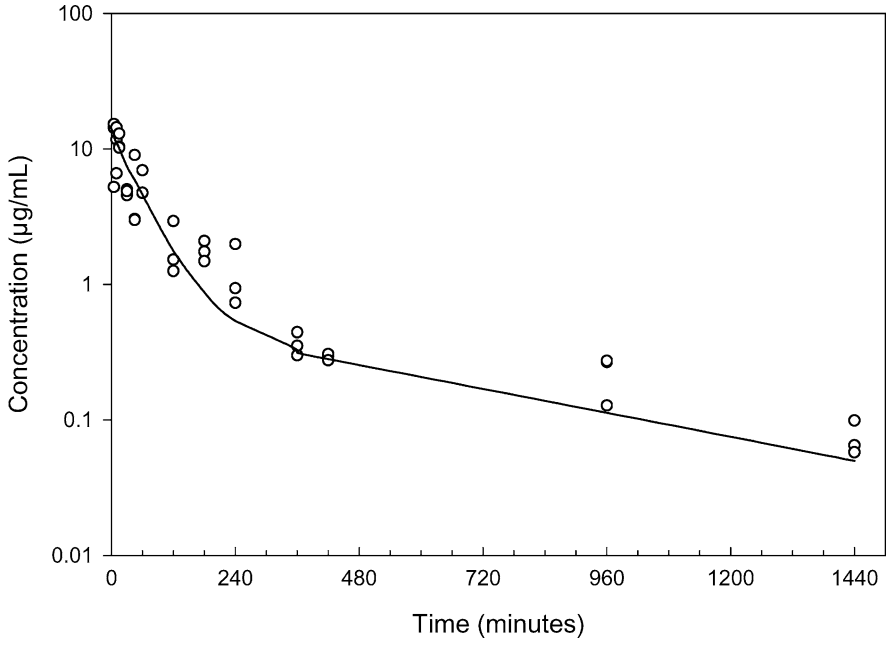

Fig. 2 Observed and predicted concentrations of FTC in plasma of SCID mice bearing T8 tumors after IV administration of 25 mg/kg FTC. *Open circles* represent the individual observed concentrations and the *solid line* indicates model-predicted concentrations

NONMEM. The inter-animal variability and 95% CI were calculated with accuracy only for the clearance term due to the low sample size. Mean clearance was estimated to be 0.55 ml/min (25.0 ml/min/kg) with a tight confidence interval (0.44–0.65 ml/min) and a 56% coefficient of variation representing the intersubject variability. Mean volume of distribution was estimated to be 41.8 ml (1907 ml/kg) with a confidence interval of 35.6–47.9 ml.

Figure 2 shows the observed FTC plasma concentrations obtained from the individual mice and the predicted concentrations obtained from the NONMEM model. A plot of the observed versus predicted FTC concentrations and weighted residuals versus predicted concentrations (Figs. 3 and 4) did not show substantial bias indicating satisfactory model fit. The area under the plasma concentration curve was calculated using the Bailer's method and the AUC_{0-1440} for FTC was 1128 µg min/ml with a 95% CI of 1093–1163 µg min/ml (Table 2). The clearance of FTC, calculated from the AUC_{0-1440} using Eq. 5 was 0.49 ml/min (22.4 ml/min/kg). This value fell within the 95% CI range of the clearance calculated by NONMEM (Table 1), thus validating the NONMEM model.

The peak plasma FTC concentrations were 11.6 ± 5.5 µg/ml at 5 min, the earliest time point sampled and the concentrations of FTC in plasma were above the lower limit of quantitation throughout the sampling period (24 h).

Tissue concentrations of FTC following IV administration

FTC was widely distributed following IV administration of 25 mg/kg FTC (Table 3). The highest concentrations were found in lung, liver and kidney in decreasing order, respectively. In liver and kidney the concentrations were maximal at 5 min (first time point) and declined progressively thereafter (Table 3). Lung concentrations were 80–100 times higher than those in plasma, liver and kidney at all time points examined and did not decline until 30 min after dosing. The concentrations of FTC in the heart, brain and skeletal muscle were found to be maximal at 5 min and were much lower at all time points than the concentrations in plasma, lung, liver and kidney. Concentrations of FTC in the fat were maximal at 15 min and in the spleen peaked at 180 min after

Table 1 Plasma pharmacokinetic parameters of FTC after IV administration to female SCID mice bearing T8 tumors at a dose of 25 mg/kg (data based on NONMEM results) (*CL* mean clearance from the central compartment, V_c volume of distribution of the central compartment, Q intercompartmental clearance, V_2 volume of the peripheral compartment, *NE* not estimated or not applicable)

Parameter	Units	Mean estimate (95% confidence interval)	Intersubject variability, % (95% confidence interval)
CL	ml/min	0.55 (0.44, 0.65)	56 (21.5, 76.1)
V_c	ml	41.8 (35.6, 47.9)	NE
Q	ml/min	0.21 (0.05, 0.36)	NE
V_2	ml	85.8 (44, 128)	NE

Table 2 Area under the curves (AUC_{0-1440}) for plasma and tissues for FTC in female SCID mice bearing T8 tumors at a dose of 25 mg/kg

Plasma/tissue	AUC_{0-1440} (μg min/ml)	95% CI	Tissue/plasma ratio
Plasma	1,128 ± 111	1,093–1,163	
Lung	446,190 ± 4,654	444,729–447,651	396
Spleen	228 ± 94	199–258	0.20
Liver	1,030 ± 103	997–1,062	0.91
Kidney	1,020 ± 144	975–1,066	0.90
Tumor	512 ± 101	480–544	0.45
Heart	242 ± 78	217–266	0.21
Brain	154 ± 55	137–172	0.14
Skeletal muscle	212 ± 81	187–238	0.19
Fat	669 ± 107	636–703	0.59

injection. The concentrations of FTC in the brain and the tumor were low (tumor was lower than the brain) and this is consistent with the presence of the blood–brain barrier and tumor blood-flow resistance, respectively [6, 11]. Tumor concentrations of FTC did not reach peak concentrations until 60 min after the injection.

The AUC_{0-1440} of FTC in tissues is presented in Table 2 along with the tissue to plasma ratio. The highest tissue to plasma ratio was found in the lung (396) followed by liver, kidney and fat. The amount of unchanged drug excreted in the urine over a period of 24 h was 1.52 μg and in the feces was 4.55 μg, which represents 0.26% and 0.82% of the total dose administered, respectively.

BCRP levels in the Igrov1/T8 tumor

Quantitative RT-PCR analysis revealed that BCRP mRNA expression in the sample tumors was not affected by FTC administration, with the levels ranging from $1.50\times10^5 \pm 7.10\times10^4$ to $1.82\times10^5 \pm 2.17\times10^5$ copies of BCRP/pg β-actin mRNA from 5 min to 24 h, respectively (Fig. 5). These levels were lower than those observed in the pure Idrov1/T8 cells grown in tissue culture. The levels in Igrov1 cells grown in tissue culture were $2.44\times10^3 \pm 119$ copies of BCRP/β-actin mRNA and those in the Igrov1/T8 cells expressing BCRP grown in tissue culture were $1.33\times10^6 \pm 4.53\times10^4$ copies of BCRP/pg β-actin mRNA (Fig. 5).

Discussion

FTC is a novel agent that completely reverses BCRP-mediated drug resistance without reversing resistance to cells that overexpress Pgp or MRP1 [18]. BCRP has been shown to have mutations that affect the substrate specificity [8] and there are reports that FTC completely inhibits both the wildtype and mutant form of BCRP expressed in *Xenopus* oocytes [15].

This study is the first in which the pharmacokinetics and tissue distribution of FTC have been investigated in vivo and its uptake in BCRP-overexpressing human ovarian cancer xenografts examined. Unlike earlier studies in which FTC caused tremors in 1-day-old cockerels when administered as an oral extract [3], the single IV dose of 25 mg/kg FTC used in the present study did not cause any long-term effects and the animals appeared normal by 4 h after administration of the dose. No gross changes were noted in any of the tissues at necropsy, 15 days after administration of the dose.

Table 3 Plasma and tissue concentrations of FTC in female SCID mice bearing T8 tumors after IV injection at a dose of 25 mg/kg (data are means ± standard deviation) (*BLD* below limit of detection)

Time (min)	Plasma (μg/ml)	Lung (μg/g)	Spleen (μg/g)	Liver (μg/g)	Kidney (μg/g)	Tumor (μg/g)	Heart (μg/g)	Brain (μg/g)	Skeletal muscle (μg/g)	Fat (μg/g)
5	11.6 ± 5.50	965 ± 607	0.39 ± 0.19	9.51 ± 5.77	9.14 ± 2.01	0.217 ± 0.14	2.18 ± 0.89	1.73 ± 0.95	1.96 ± 0.68	0.62 ± 0.26
10	10.9 ± 3.97	741 ± 590	0.58 ± 0.13	7.32 ± 2.34	8.10 ± 3.20	0.45 ± 0.30	1.80 ± 0.90	0.84 ± 0.50	0.80 ± 0.30	1.80 ± 0.60
15	11.2 ± 1.55	1078 ± 225	0.68 ± 0.20	8.43 ± 3.00	5.70 ± 1.70	0.33 ± 0.12	1.40 ± 0.30	0.83 ± 0.30	1.40 ± 0.30	2.80 ± 0.50
30	4.81 ± 0.23	469 ± 63.1	0.46 ± 0.17	4.10 ± 1.40	3.50 ± 0.90	0.44 ± 0.20	0.90 ± 0.20	0.40 ± 0.20	0.60 ± 0.04	1.90 ± 0.80
45	5.00 ± 3.45	935 ± 442	0.52 ± 0.50	3.12 ± 1.90	3.90 ± 4.00	0.72 ± 0.35	0.70 ± 0.50	0.40 ± 0.20	0.70 ± 0.90	2.60 ± 1.20
60	5.46 ± 1.28	1301 ± 351	0.51 ± 0.10	3.30 ± 0.40	4.00 ± 1.00	1.00 ± 0.90	0.70 ± 0.30	0.50 ± 0.10	0.90 ± 0.30	3.60 ± 1.30
120	1.89 ± 0.89	532 ± 387	0.37 ± 0.20	3.20 ± 1.00	1.80 ± 1.20	0.40 ± 0.09	0.50 ± 0.03	0.50 ± 0.50	0.30 ± 0.14	0.92 ± 0.70
180	1.77 ± 0.31	832 ± 62.3	0.95 ± 0.47	2.90 ± 1.90	2.00 ± 0.30	0.70 ± 0.30	0.60 ± 0.25	0.22 ± 0.07	0.40 ± 0.13	1.20 ± 0.40
240	1.22 ± 0.67	167 ± 61.7	0.35 ± 0.17	2.10 ± 0.80	1.10 ± 0.70	0.90 ± 0.60	0.30 ± 0.10	0.20 ± 0.20	0.20 ± 0.05	0.44 ± 0.20
360	0.364 ± 0.07	145 ± 144	0.23 ± 0.40	1.00 ± 0.70	0.40 ± 0.20	0.50 ± 0.40	0.10 ± 0.05	0.15 ± 0.20	0.07 ± 0.03	0.20 ± 0.20
420	0.295 ± 0.02	153 ± 33.1	0.11 ± 0.20	0.14 ± 0.08	0.30 ± 0.20	0.80 ± 0.70	0.20 ± 0.10	0.04 ± 0.02	0.15 ± 0.15	0.21 ± 0.06
960	0.22 ± 0.08	348 ± 206	0.03 ± 0.010	BLD	0.30 ± 0.09	0.30 ± 0.10	0.04 ± 0.02	0.03 ± 0.003	0.04 ± 0.01	0.30 ± 0.06
1440	0.07 ± 0.02	108 ± 76.1	BLD	BLD	0.20 ± 0.07	0.20 ± 0.20	BLD	0.02 ± 0.001	0.02 ± 0.002	0.10 ± 0.03

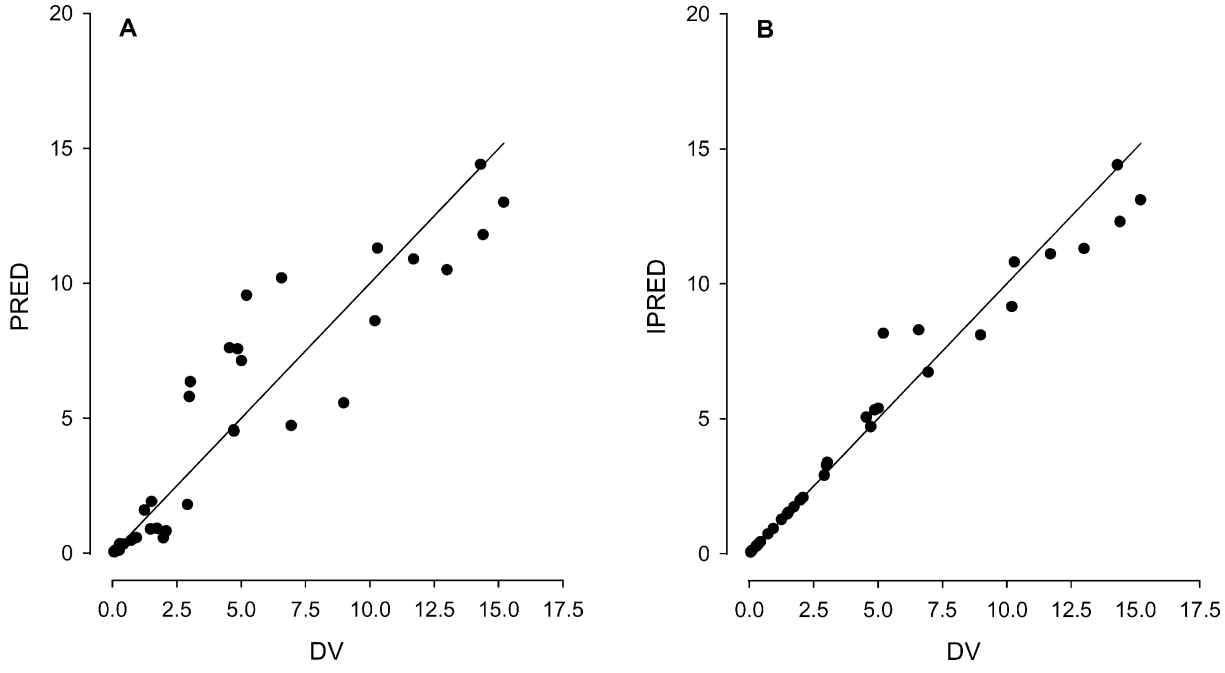

Fig. 3 Observed plasma concentrations (DV) plotted as a function of (**a**) population-predicted (PRED) and (**b**) individual predicted (IPRED) plasma concentrations of FTC. The *closed circles* are the individual data and the *lines* are the unity lines

The aim of using mice bearing tumors was to evaluate the FTC penetration into the tumor and also to evaluate whether FTC affected the BCRP levels in the tumor.

The plasma time-course of FTC was best described by a two-compartment model using NONMEM. There was no significant reduction in the AIC when a three-compartment model, as compared to a two-compartment model, was fit to the data. The clearance of FTC was calculated to be 0.55 ml/min with an intersubject variability of 56%. As clearance is a relevant physiologic parameter these data may be of use in other studies in which FTC is studied in vivo or when the effect of FTC is being studied in other BCRP substrates to achieve adequate levels of FTC. Less than 2% of the administered dose was accounted for in urine and feces at 24 h, suggesting hepatic metabolism as the primary mechanism of elimination of FTC. Preliminary studies in our laboratory (data not shown) suggest metabolism by cytochrome P450 3A4 as one likely mechanism for FTC elimination.

The highest concentrations in plasma (approximately 26–30 μM) were observed at the first sampling time of

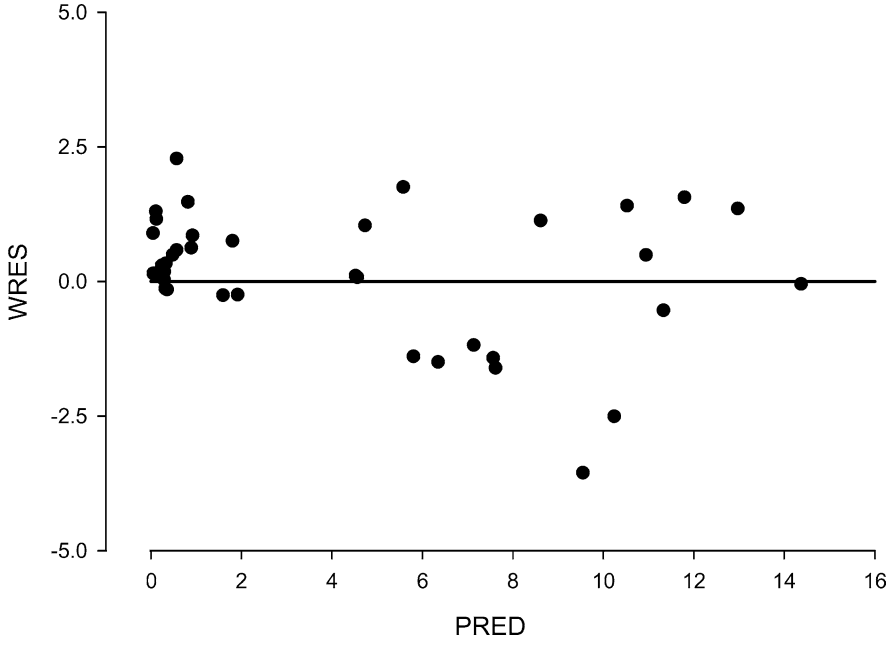

Fig. 4 Weighted residuals (WRES) versus predicted concentrations (PRED) for the pharmacokinetic model of FTC after administration of 25 mg/kg to female SCID mice bearing T8 tumors. The *closed circles* are the individual data

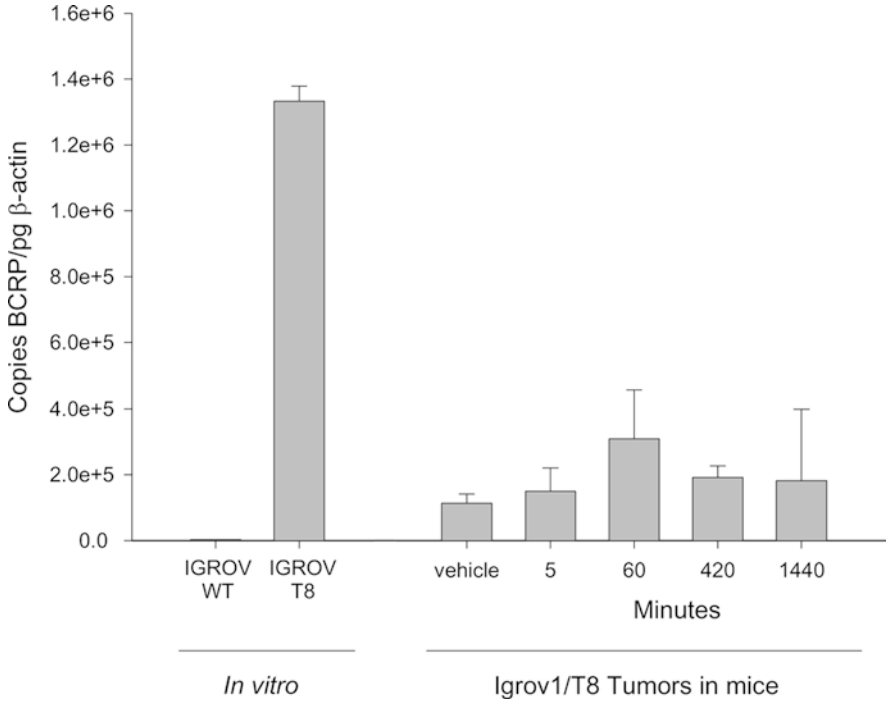

Fig. 5 Levels of BCRP as measured by RT-PCR using a thermal light cycler in the control IGROV cells, T8 IGROV cells expressing BCRP and the T8 tumor excised from the control or treated mice at 5, 60, 420, and 1440 min after FTC dosing. The levels of BCRP are expressed as copies of BCRP/pg of β-actin

5 min after injection. These concentrations were approximately 6–30 times higher than the FTC concentration range required (1–5 μM or 0.38–1.9 μg/ml) to cause reversal of BCRP-mediated resistance [19] and remained above that FTC concentration for approximately 360 min (6 h) after injection. However, whether these plasma levels of FTC could be extrapolated to in vivo BCRP reversal requires further investigation with special emphasis on protein binding of FTC and high serum conditions in vitro.

FTC was widely distributed in mouse tissues and was measurable at 24 h after dosing, the last time point sampled, in all the tissues sampled except spleen, liver and heart. Taking into view the wide tissue distribution of BCRP [13], the current results emphasize the usefulness of FTC as a BCRP inhibitor. FTC levels in liver, which expresses high BCRP levels, remained above 2 μg/ml for 4 h after administration. The highest concentrations were found in the lung with levels approximately 80 times higher than the highest plasma concentrations. These high concentrations were sustained for the entire sampling period and suggest a depot effect in the lung. FTC probably binds extensively to lung tissue which could be magnified by the lung first pass effect following IV dosing. As can be seen in Table 3,around 40% of the administered dose is found in the lungs initially. This could explain the short-term respiration problems that were observed in the FTC-dosed animals. However, whether the high concentrations of FTC in the lung have any bearing on the available dose/amount of FTC in other tissues requires further study of FTC administered either intraperitoneally or orally.

The presence of BCRP has been demonstrated in both normal human brain and intracranial tumors and it has been localized to the blood–brain barrier, mainly at the luminal surface of microvessel endothelium [4]. This localization of BCRP is similar to that of Pgp. Brain concentrations of FTC were about one-tenth the concentrations in plasma. However, the brain concentrations of FTC remained above 1 μ*M* for 2 h and these concentrations of FTC are high enough to cause short-term BCRP reversal. Whether this inhibition of BCRP will be sufficient to alter concentrations of key BCRP substrates in the brain is open to investigation. However, because BCRP shares several substrates in common with Pgp our results and previously reported results [4] suggest that BCRP may serve as an additional blockade at the blood–brain barrier in normal tissues and intracranial tumors.

BCRP has the potential to play an important role in tumor transport of certain drugs including mitoxantrone, and camptothecin-based anticancer drugs, such as topotecan and SN-38, the active metabolite of irinotecan [17]. FTC administration did not appear to cause a significant difference in the expression of BCRP mRNA in the tumors as measured by RT-PCR, which indicates that FTC causes BCRP reversal without affecting BCRP mRNA expression. However, BCRP mRNA expression in tumor tissue was less than that in Igrov1/T8 cells grown in tissue culture. This is likely the result of the presence of non-BCRP-expressing cells in the tumor tissue such as stromal and vascular cells and due to variation from a plastic to an in vivo model system.

The FTC concentrations in the tumors remained above 1 μ*M* (0.38 μg/ml), which is required for BCRP inhibition, for the 24-h sampling period (Table 3), indicating that FTC attains sufficient concentrations in the tumor to cause BCRP reversal based on in vitro cell models. Whether this is sufficient to overcome resistance

to BCRP-transported drugs in tumor in vivo awaits further investigation.

The data presented in this report demonstrate that FTC can be administered IV to tumor-bearing mice as a single 25 mg/kg dose without severe toxicity. After administration, FTC is widely distributed to tissues, including brain and tumor where it is thought that BCRP plays a role maintaining a barrier for drug penetration. This study provides a basis for future in vivo studies designed to investigate the impact of BCRP on drug resistance and the utility of FTC and its analogues to be useful BCRP inhibitors.

Acknowledgement This work was supported in part by a Department of Veterans Affairs Merit Review Grant (Dr Ross).

References

1. Allen JD, Brinkhuis RF, Wijnholds J, Schinkel AH (1999) The mouse Bcrp1/Mxr/Abcp gene: amplification and overexpression in cell lines selected for resistance to topotecan, mitoxantrone, or doxorubicin. Cancer Res 59:4237–4241
2. Bailer AJ (1988) Testing for the equality of area under the curves when using destructive measurement techniques. J Pharmacokinet Biopharm 16:303–309
3. Cole RJ, Cox RH, Tremorgen Group (1981) Handbook of toxic fungal metabolites. Academic Press, New York, pp 355–509
4. Cooray HC, Blackmore CG, Maskell L, Barrand MA (2002) Localisation of breast cancer resistance protein in microvessel endothelium of human brain. Neuroreport 13:2059–2063
5. Doyle LA, Yang W, Abruzzo LV, Krogmann T, Gao Y, Rishi AK, Ross DD (1998) A multidrug resistance transporter from human MCF-7 breast cancer cells. Proc Natl Acad Sci USA 95:15665–15670
6. Hazlehurst LA, Foley NE, Gleason-Guzman MC, Hacker MP, Cress AE, Greenberger LW, De Jong MC, Dalton WS (1999) Multiple mechanisms confer drug resistance to mitoxantrone in the human 8226 myeloma cell line. Cancer Res 59:1021–1028
7. Honjo Y, Hrycyna CA, Yan QW, Medina-Perez WY, Robey RW, van de Laar A, Litman T, Dean M, Bates SE (2001) Acquired mutations in the MXR/BCRP/ABCP gene alter substrate specificity in MXR/BCRP/ABCP-overexpressing cells. Cancer Res 61:6635–6639
8. Janvilisri T, Venter H, Shahi S, Reuter G, Balakrishnan L, van Veen HW (2003) Sterol transport by the human breast cancer resistance protein (ABCG2) expressed in *Lactococcus lactis*. J Biol Chem 278:20645–20651
9. Jonker JW, Buitelaar M, Wagenaar E, Van Der Valk MA, Scheffer GL, Scheper RJ, Plosch T, Kuipers F, Elferink RP, Rosing H, Beijnen JH, Schinkel AH (2002) The breast cancer resistance protein protects against a major chlorophyll-derived dietary phototoxin and protoporphyria. Proc Natl Acad Sci U S A 99:15649–15654
10. el-Kareh AW, Secomb TW (1997) Theoretical models for drug delivery to solid tumors. Crit Rev Biomed Eng 25:503–571
11. Kristjansen PE, Brown TJ, Shipley LA, Jain RK (1996) Intratumor pharmacokinetics, flow resistance, and metabolism during gemcitabine infusion in ex vivo perfused human small cell lung cancer. Clin Cancer Res 2:359–367
12. Kruijtzer CM, Beijnen JH, Rosing H, ten Bokkel Huinink WW, Schot M, Jewell RC, Paul EM, Schellens JH (2002) Increased oral bioavailability of topotecan in combination with the breast cancer resistance protein and P-glycoprotein inhibitor GF120918. J Clin Oncol 20:2943–2950
13. Maliepaard M, van Gastelen MA, de Jong LA, Pluim D, van Waardenburg RC, Ruevekamp-Helmers MC, Floot BG, Schellens JH (1999) Overexpression of the BCRP/MXR/ABCP gene in a topotecan-selected ovarian tumor cell line. Cancer Res 59:4559–4563
14. Maliepaard M, Scheffer GL, Faneyte IF, van Gastelen MA, Pijnenborg AC, Schinkel AH, van De Vijver MJ, Scheper RJ, Schellens JH (2001) Subcellular localization and distribution of the breast cancer resistance protein transporter in normal human tissues. Cancer Res 61:3458–3464
15. Nakanishi T, Doyle LA, Hassel B, Wei Y, Bauer KS, Wu S, Pumplin DW, Fang HB, Ross DD (2003) Functional characterization of human breast cancer resistance protein (BCRP, ABCG2) expressed in the oocytes of Xenopus laevis. Mol Pharmacol 64:1452–1462
16. Nakanishi T, Karp JE, Tan M, Doyle LA, Peters T, Yang W, Wei D, Ross DD (2003) Quantitative analysis of breast cancer resistance protein and cellular resistance to flavopiridol in acute leukemia patients. Clin Cancer Res 9:3320–3328
17. Nakatomi K, Yoshikawa M, Oka M, Ikegami Y, Hayasaka S, Sano K, Shiozawa K, Kawabata S, Soda H, Ishikawa T, Tanabe S, Kohno S (2001) Transport of 7-ethyl-10-hydroxycamptothecin (SN-38) by breast cancer resistance protein ABCG2 in human lung cancer cells. Biochem Biophys Res Commun 288:827–832
18. Rabindran SK, He H, Singh M, Brown E, Collins KI, Annable T, Greenberger LM (1998) Reversal of a novel multidrug resistance mechanism in human colon carcinoma cells by fumitremorgin C. Cancer Res 58:5850–5858
19. Rabindran SK, Ross DD, Doyle LA, Yang W, Greenberger LM (2000) Fumitremorgin C reverses multidrug resistance in cells transfected with the breast cancer resistance protein. Cancer Res 60:47–50
20. Robey RW, Medina-Perez WY, Nishiyama K, Lahusen T, Miyake K, Litman T, Senderowicz AM, Ross DD, Bates SE (2001) Overexpression of the ATP-binding cassette half-transporter, ABCG2 (Mxr/BCrp/ABCP1), in flavopiridol-resistant human breast cancer cells. Clin Cancer Res 7:145–152
21. Sikic BI (1999) Modulation of multidrug resistance: a paradigm for translational clinical research. Oncology (Huntingt) 13:183–187